Received: 6 October 2023 | Revised: 2 January 2024 | Accepted: 18 January 2024

DOI: 10.1111/jace.19735

Journal of the American Ceramic Society

RAPID COMMUNICATION

Current rate flash sintering of nickel at ambient temperature in <1 min

Emmanuel A. Bamidele[1] | **Morsi M. Mahmoud**[3,4] | **Rishi Raj**[1,2]

[1]Materials Science and Engineering Program, University of Colorado, Boulder, Colorado, USA

[2]Department of Mechanical Engineering, University of Colorado, Boulder, Colorado, USA

[3]Mechanical Engineering Department, College of Engineering and Physics, King Fahd University of Petroleum and Minerals, Dhahran, Saudi Arabia

[4]Interdisciplinary Research Center for Advanced Materials, King Fahd University of Petroleum & Minerals, Dhahran, Saudi Arabia

Correspondence
Rishi Raj, University of Colorado, Boulder, CO 80309, USA.
Email: rishi.raj@colorado.edu

Morsi M. Mahmoud is on sabbatical leave from Fabrication Technology Department, Advanced Technology and New Materials Research Institute (ATNMRI), City for Scientific Research and Technological Applications (SRTA), New Borg Al-Arab City, P.O. Box: 21934, Alexandria, Egypt.

Funding information
Ames Research Center, Grant/Award Number: 80NSSC21K0225

Abstract

We show that powder pressed specimens of nickel can be sintered to 99.96% density by injecting electrical current, without the use of a furnace. Full sintering could be accomplished in 10 to 52 s by changing the current rate from 5 to 1 A/s. In all instances, the samples sintered abruptly at a current density of ~20 A mm^{-2}. The grain size of the sintered samples was somewhat larger than the nickel powder particle size (~60 μm vs. 40 μm). Tensile testing yielded a yield strength of 98 MPa, ultimate tensile stress of 323 MPa, and ductility of ~17%. Four in-operando measurements are reported: (i) sintering, (ii) the change in resistance with current density, (iii) the temperature, and (iv) electroluminescence. The change in resistance during flash sintering exhibited a high peak followed by a steep decline in resistance; the transient is attributed to the breakdown of particle–particle interface resistance. The same cycle repeated with the flash-sintered, dense sample, did not show the spike, and gave reproducible results. The resistance data for these latter cycles, when viewed as a function of temperature exhibited sigmoidal behavior: initially lower, and then higher than the literature values. This unusual behavior reflects the influence of defects generated during flash. We have also measured the endothermic enthalpy, expressed by the difference between the in situ input electrical energy and the radiation, convection, and specific heat losses. Dividing by the formation energy of Frenkel pairs yields the concentration of defects, estimated to be 0.3–0.4 mol %. These concentrations are far above thermal equilibrium; it is concluded that flash of metals is a far from equilibrium phenomenon.

KEYWORDS
current rate, electro-discharge sintering, flash sintering, nickel

1 | INTRODUCTION

Flash sintering of ceramics was discovered in 2010.[1] It was shown that many ceramics, ionic conductors, semiconductors, ferroelectrics, and insulators[2] could be sintered in this way. It was not obvious that electronic conductors, that is, metals, too could be flash-sintered. However, recently we have shown that tungsten can be sintered in a few seconds at 1000°C by the flash method. Although ceramics required auxiliary heating with a furnace, tungsten could be sintered without a furnace by injecting current directly into the dog bone specimens and increasing it at a constant rate.

(Current-rate flash sintering of metals bears similarity to electro-discharge-sintering (EDS)[4] where a large amount of energy stored in a capacitor is dumped within a

millisecond into a powder-pressed sample of a metal, causing it to sinter. The present experiments are qualitatively similar, except that current is increased gradually over a period of several seconds to cause sintering. The flash experiments offer much greater control; slowing down the current rate allows time for in-operando measurements of the flash behavior. We report continuous measurements of sintering, temperature, electroluminescence, and resistivity. These data can provide insights into the role of defects in flash sintering of metals. The time scale of EDS and flash differs by many orders of magnitude. The ultrashort time scale of EDS does not permit measurements of the change in resistance or the advent or electroluminescence, which are key features of flash. Therefore, the equivalence between EDS and flash sintering of metals remains speculative. We hope that in the future, the chasm between the sub-millisecond time scale of EDS and several seconds long time scale of flash can be bridged; perhaps, existing EDS systems can be expanded to include flash protocols.)

The present results on Ni, a main group metal, are similar to recent results on tungsten (W), a refractory metal. These results, taken together, are starting to show general phenomenological behavior of flash sintering in metals.

The present work is an important development in the science and technology of sintering. The simplicity of the point defects, vacancies, and interstitials, in metals may lead to an easier path for understanding the fundamental mechanism(s) of the flash phenomenon. It may also have technological impact: For example, in situ additive manufacturing where digital build up can be integrated with flash sintering to produce parts that are end-user ready.

Flash is immensely more energy efficient than conventional sintering. Instead of large inefficient furnaces, flash can be carried out with table-top systems with a small footprint. The injection of energy directly into the workpiece for sintering sidesteps the energy-wasting inefficiency of large furnaces that operate at very high temperature, possibly revolutionizing the way materials will be sintered in the future. We foresee flash enabling electrification of materials manufacturing.

2 | METHODS

The flash-sintering experiments were carried out within a glove box (<100 ppm O_2), without a furnace, by injecting DC electrical current directly into dog bones, as in tungsten.[3] The current was raised at a constant rate until the workpiece sintered. The open architecture of the experiment allowed full access to the specimen: a camera measured sintering strain, a pyrometer measured the temperature, and a spectrometer characterized the optical emission spectrum.

The dog bone specimens were pressed into shape from Ni powder, obtained from Alfa Aesar. They were specified to be 99.8% pure with an average particle size of 44 μm. The die was filled with about 1.5 g of powder and pressed with 150 and 180 MPa, yielding specimens with a gage length of 20 mm, a width of 3.55 mm, and a thickness of 0.71 mm. The green density of these samples was 85%–87%.

One-millimeter holes were drilled into the ends of the dog bone specimen. Electrodes made from tungsten were inserted into them to supply electrical current, from a KEPCO KLN 30-100 power supply. Two more holes at the outer edges of the gage length, just inside from current carrying electrodes were drilled to measure the voltage. This voltage measurement, which does not draw any current, and the current injected from the outer electrodes were used to measure the "four-point" resistance from the *I*–*V* curve obtained in this way.

The specimen temperature was measured with a CTLM-1HCF4-C3 pyrometer from Micro-Epsilon (USA); the emissivity was set to 0.12.[5] The optical emission spectra were recorded with an Ocean Optics spectrometer (model USB4000-UV–VIS), which was connected to a Spectra Suite. The outputs from the power source (i.e., the current), the voltmeter, the pyrometer, the spectrometer, and the software for controlling the current rate were interfaced to a computer via an NI DAQ card. A video camera recorded images, which were analyzed for shrinkage.

3 | RESULTS

3.1 | Sintering

Sintering was carried out at three current rates: 1, 2, and 5 A/s. The shrinkage curves are shown in Figure 1A. The samples sintered in 52, 26, and 10 s respectively. The sintering data merged into a common curve when plotted against the instantaneous values of the current density, as shown in Figure 1b. Similar behavior was seen in flash sintering of W[3], and earlier in flash sintering of yttria stabilized zirconia.[6] Collectively these results prove that current density is the critical parameter that controls the shrinkage in flash experiments. The fundamental mechanism for this behavior is not understood, although they resemble experiments with ceramics, where it was shown that the extent of sintering was related simply to the current density limit placed at the power supply.[7]

The sintered density estimated from the equation $\rho_g = \rho\exp(3\epsilon_1)$,[8] where ρ_g is the green density, ρ is the final density, and ϵ_1 is the linear shrinkage strain (note that it is a negative quantity). Thus, shrinkage strain of 0.045 and a green density of 86% yields >99% for the final density. Archimedes measurements yielded 99.6% relative density.

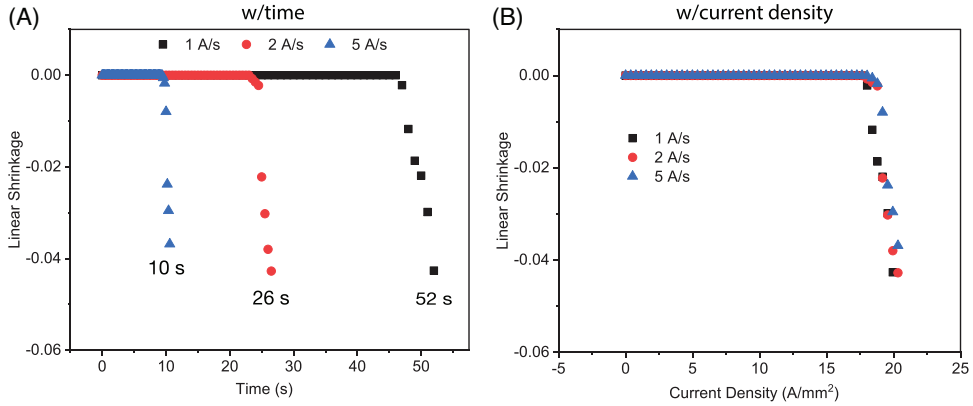

FIGURE 1 (A) Linear shrinkage measured from the video captured using a CCD camera, at three current rates. The video images were analyzed for shrinkage using Fiji software. (B) Same data where the shrinkage is plotted as a function of the current density.

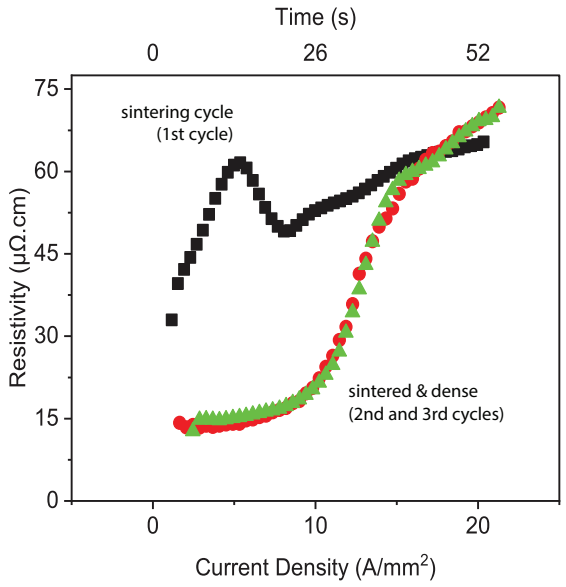

FIGURE 2 Resistivity as a function of current density and time during the first cycle of the flash sintering experiment (black). The other two datasets were obtained by re-flashing the specimen after the first cycle. The first cycle data are for powder specimen and the latter two for dense sample.

3.2 | Three cycles

The resistance measured as a function of the current density is shown in Figure 2. The measurements were made in three cycles. In the first cycle the specimen was the initial powder pressed dog bone. During the second and third cycles the sample that had been sintered to full density during the first cycle was subjected again to two more flash cycles. These latter cycles show the influence of the flash effect on the resistance of a dense sample: The resistance is low at first but then rises to catch up with the resistance measured during the first sintering cycle.

The transient peak in the first cycle was also seen in tungsten. Even earlier it had been observed in field assisted experiments with aluminum powders[9]—although those experiments were not ascribed to "flash." The transient is attributed to the breakdown of the interfacial resistance between particles. The resistance profile in cycles 2 and 3 is unusual, where it is compared to the handbook values of the temperature dependent resistance of Ni.

3.3 | Temperature and luminescence

The temperature of the specimen measured with a pyrometer, as well as the luminescence spectrum, are shown in Figure 3.

The luminescence is ascribed to electroluminescence, rather than to black body radiation, for two reasons. (i) The temperatures are too low for strong optical emission just from Joule heating and (ii) The emission peak increases in intensity but remains at the same position when the specimen temperature increases. In BBR the emission peak moves to shorter wavelengths as temperature rises.

Curiously the emission spectra are similar to the emission from ceramics.[10] It is likely that the flash induced plasma ionizes the atmospheric gas, which dominates the emission spectrum.

3.4 | The resistivity

The in-operando resistance was measured by the four-point method as described in Section 2. Three sets of data are reported in Figure 4. (i) The in-operando resistance during flash measured without furnace heating—in purple, (ii) resistance of the post-flash specimen, now fully dense, measured without injecting current but now

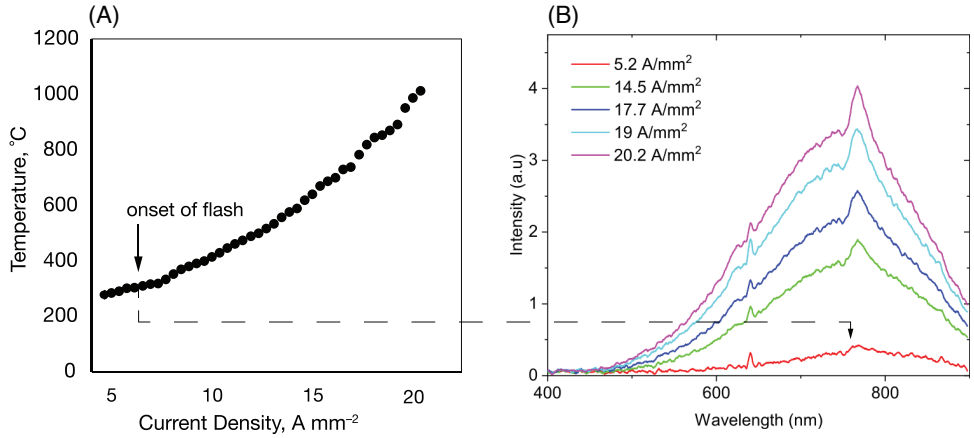

FIGURE 3 (A) Temperature as measured with a pyrometer as a function of the current density. (B) Electroluminescence spectra as a function of the current density. The current density increases the temperature and therefore the intensity of photoemission. Note that the position of the emission peak does not shift with temperature. The onset of flash is related to the onset of photoemission.

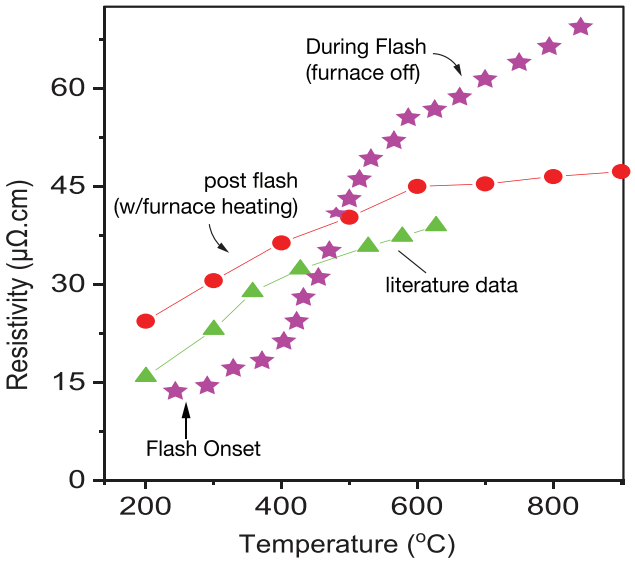

FIGURE 4 Resistivity behavior during flash and with furnace heating of the flash sintered specimen. The temperature dependent resistivity data from literature are shown in red color.

heated with a furnace (orange), and (iii) handbook data from the literature[11] (shown in green).

The following features of Figures 3 and 4 are notable:

(i) The furnace-heating resistivity data of dense samples (prepared by flash sintering) are comparable to the literature data. The magnitude is a bit higher (which can be ascribed to residual defects) but the trend is consistent.

(ii) The in-operando resistance during the second and third flash cycles of the dense specimen is remarkably different from post flash behavior, as described just above. At first the resistance is lower than the handbook values but then increases with temperature in a sigmoidal fashion. These differences may not be ascribed to porosity as these data are for dense samples. The shape, therefore, reflects the influence of the defects. The drop in resistance below the handbook values (in the lower temperature range) corresponds to the rise in (electronic) conductivity that is a characteristic of flash in ceramics.[7]

(iii) The electroluminescence spectra given in Figure 3 reflect the generation of photons. Curiously these spectra are similar to those obtained in ceramics,[10] which suggests that the electroluminescence may be a near surface phenomenon rather than a matrix effect, as has been assumed in earlier papers from this laboratory. The high electronic conductivity probably plays a role in the generation of such a surface plasma.

3.5 | Defect generation and mechanical behavior

The tensile stress–strain curve is given in Figure 5A. It gives a yield stress of about 98 MPa, an ultimate tensile stress of 323 MPa and ductility of ~17%.

The fracture micrograph is given in Figure 5B. Curiously, it shows a dimpled fracture surface, which is typical of dispersion strengthened metals[12]; for example, in copper, nanoscale oxide particles of alumina become sites for cavity nucleation, which leave behind a dimpled surface.[13] The particles concentrate the plastic strain; voids nucleate and grow to cause ductile fracture. The surprising result in present experiments is that the dimples form without a dispersion.

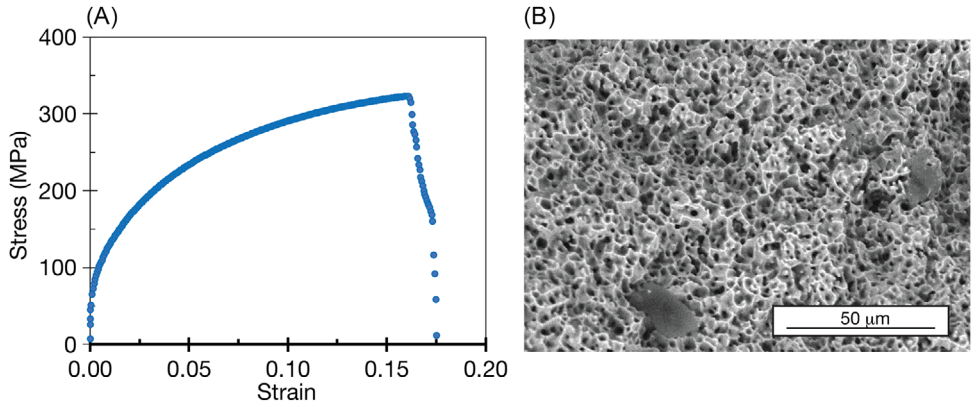

FIGURE 5 (A) Tensile stress–strain curve for the flash sintered nickel specimen and (B) an SEM micrograph showing a dimpled fracture surface.

In Supporting Information, we describe the measurement of endothermic enthalpy during flash sintering from the difference between the input electrical energy and the energy lost to black body and convective losses, and the enthalpy stored as specific heat. The difference when converted into the concentration of defects (Frenkels: vacancy–interstitial pairs) gives values of 0.3%–0.4% mole fraction of Frenkel pairs at specimen temperature of ~900°C. This value is several orders of magnitude greater than the concentrations expected from thermal equilibrium. It is proposed that the defects form "stiff" clusters that resist deformation and thus become the source of void nucleation, as in copper.[12]

4 | DISCUSSION

This is the second report on flash sintering of metals, namely, Ni. The first was on tungsten powders,[14] a highly refractory metal. Ni melts as 1455°C, whereas the melting point of W is 3383°C. In classical solid-state diffusion, the diffusion coefficient scales with the melting point of the metal.[15] Normally diffusion rates that occur at $0.75T_M$ are needed for sintering within a few hours. Therefore, conventional sintering of tungsten requires much higher temperatures (~2450°C) than NI (~1023°C). However, in flash experiments both metals sinter to full density near 1000°C. It is therefore self-evident that mass transport during flash is quite apart from conventional solid-state diffusion: It is a far from equilibrium phenomenon.

Diffusion rates in flash have been compared with conventional solid-state diffusion in recent experiments where bilayers of zirconia and lanthana were flashed and the progression of the interfacial reaction (to form lanthanum zirconate) was measured as a function of time and temperature.[16] These experiments suggest cation diffusion to be nearly $\times 10^8$ faster in flash than nominal diffusion rates. Moreover, the activation energy for diffusion is one half to one third of the literature values, not only in these diffusion measurements but also in superplastic deformation during flash.[17] Recent experiments where the superimposition of magnetic fields was shown to migrate the flash from a dog bone sample into a free standing workpiece without electrical contacts[18] suggest that flash is akin to solid-state plasma. However, in-operando experiments at synchrotrons have shown that the crystal structure of the solid remains intact during flash, suggesting the plasmas, as postulated here, arise from the high electronic conductivity induced by flash near the surface of the specimens. Much remains to be explored in this exciting new development.

It seems that the rate of mass transport can be enhanced in metals as they have been shown to be in ceramics,[16] but to what extent is currently not known.

In situ calorimetry has been employed in ceramics[19] and in our experiments with W and now in Ni (as described in full detail in Supporting Information). In these experiments the difference between input energy (electrical) and the energy lost to radiation, convection, and specific heat is measured. The deficit is assumed to reflect the endothermic generation of defects, which are estimated quantitatively. These concentrations are far above thermal equilibrium values. However, in Ni they are nearly two orders of magnitude lower than in tungsten: that is, 0.002 versus 0.2 mol fraction. This difference may be explained by the higher homologous temperature in Ni than in tungsten during flash—in both cases the pyrometer temperature is near 1000°C, which corresponds $0.74T_M$ for the case of Ni, but only $0.35T_M$ for W. We propose that the much lower homologous temperature for W prevents recombination of vacancies and interstitials, thereby leading to much higher steady-state defect concentrations in W than in Ni.

A constant feature of flash in ceramics, which are insulators, is a transition to high conductivity which is electronic in nature.[20,21] That appears to happen in metals as well,

although not so starkly as in ceramics as metals are intrinsic electronic conductors. The higher conductivity in metals at the onset of flash is reflected in the resistance profile for Ni with rising temperature (or current density), as seen in Figure 4. The resistivity falls distinctly below the handbook values[11] near the onset of flash, which reflects the increase in conductivity during flash. But as the current is increased further, the resistance begins to rise in a sigmoidal profile, which is different from the behavior of insulating ceramics where the conductivity continues to fall with increasing current.

Thus, two questions arise anew in flash of metals both related to the resistivity profile with respect to temperature. In both Ni and W, the shape of the curves is sigmoidal, consisting of three phases. At first (phase I), at the onset of flash the resistance remains flat but then, in phase II, rises sigmoidally as the temperature increases, eventually flattening again at even higher temperatures (phase III). The first and second phases are evident in Ni in Figure 4; all three phases are evident in W experiments[3] (see Figures 4B and 9D in this reference). The two metals differ in the relative magnitude of the resistivity with respect to the handbook values for Ni[11] and for W.[22] The in-flash resistance during phase I is lower than the handbook values in the case of Ni but higher for W. Nevertheless, the shape of the resistance profile is the same for both metals. We suggest that the relative magnitude of the resistivity may be related to the generation and recombination of defects, the first being related to the flash effect and the latter to the homologous temperature, which is much higher for Ni.

It is to be emphasized that the sigmoidal shape of the resistance profile, now confirmed for two metals, is likely a general feature of flash in metals, and needs to be explored fundamentally, most likely in terms of defect generation and recombination.

At the risk of being speculative, we wish to suggest that the defects during flash form patterns that affect the scattering of electrons, which may increase (Ni) or reduce (W) the electronic conductivity. In this regard the fracture micrograph in Figure 5B is interesting; the dimpled fracture surface suggests nucleation of voids as in dispersion strengthened metals. It is conjectured that defects form clusters that are difficult to deform, and which, therefore, serve as the sites for cavity nucleation. The clustering may be a sign of the way defects can alter the scattering of electrons during conduction.

5 | CONCLUSIONS

The experiments on flash sintering of W and now Ni provide interesting common features despite a wide difference between their melting points, which are 3383 and 1453°C. Both metals sinter at 1000°C. Both show a sigmoidal behavior in the resistance profile with respect to temperature. It consists of three phases, initially the profile is nearly flat, then rises sigmoidally and then tends to flatten again at higher temperatures. The phenomenological evidence suggests that this behavior is related to the generation and recombination of defects such as Frenkel pairs. The quasi steady-state concentration of the defects is much higher in W than in Ni, probably reflecting the much higher homologous temperature during flash in Ni than in W. The higher homologous temperature is expected to increase the rate of recombination thereby reducing the steady state defect concentration in Ni.

The dimpled fracture surface of the flashed specimens suggests the presence of nanoscale clusters that resist deformation and serve as nucleation sites for cavities.

Apart from the new scientific questions raised above flash sintering of metals may create new technological opportunities. For example, in situ additive manufacturing of metal workpieces that do not require further sintering can be produced.

In ceramics, reactive flash sintering of elemental oxide powders that grow into a single phase multicomponent ceramic with unusual properties has been demonstrated.[23,24] A similar approach applied to high-entropy metals and other alloys designed for super-mechanical properties produced by unusual precipitation strengthening may be feasible.

EDS of metals is already used in powder consolidation of metals. Therefore, it may be possible to graft sintering protocols on to EDS systems. That would enable the commercialization of the flash method, and perhaps, also, increase the versatility of the EDS method.

ACKNOWLEDGMENTS

This work was supported by a grant from NASA, ESI Program under the grant number 80NSSC21K0225. Lively discussions with Dr. Jhonathan Rosales (at NASA) and his encouragement as the work progressed is gratefully acknowledged. We are grateful to the King Fahd University of Petroleum and Minerals, Dhahran, 31261, Saudi Arabia for supporting Dr. Morsi Mohammed's visit to the Raj's lab at the University of Colorado Boulder to participate in this study.

ORCID

Morsi M. Mahmoud https://orcid.org/0000-0002-4602-6084

Rishi Raj https://orcid.org/0000-0001-8556-9797

REFERENCES

1. Cologna M, Rashkova B, Raj R. Flash sintering of nanograin zirconia in<5 s at 850 C. J Am Ceram Soc. 2010;93:3556–59.

2. Raj R. Analysis of the power density at the onset of flash sintering. J Am Ceram Soc. 2016;99:3226–32.
3. Bamidele E, Jalali SIA, Weimer AW, Raj R. Flash sintering of tungsten at room temperature (without a furnace) in <1 min by injection of electrical currents at different rates. J Am Ceram Soc. 2024;107:817–29.
4. Yurlova MS, Demenyuk VD, Lebedeva LY, Dudina DV, Grigoryev EG, Olevsky EA. Electric pulse consolidation: an alternative to spark plasma sintering. J Mater Sci. 2014;49:952–85.
5. Francl J, Kingery WD. Thermal conductivity: IX, experimental investigation of effect of porosity on thermal conductivity. J Am Ceram Soc. 1954;37:99–107.
6. Kumar PMK, Yadav D, Lebrun J, Raj R. Flash sintering with current rate: a different approach. J Am Ceram Soc. 2019;102:823–35.
7. Francis JSC, Raj R. Influence of the field and the current limit on flash sintering at isothermal furnace temperatures. J Am Ceram Soc. 2013;96:2754–58.
8. Raj R. Separation of cavitation-strain and creep-strain during deformation. J Am Ceram Soc. 1982;65:C-46–C-46. https://ceramics.onlinelibrary.wiley.com/doi/abs/10.1111/j.1151-2916.1982.tb10397.x
9. McWilliams B, Yu J, Kellogg F, Kilczewski S. Enhanced sintering kinetics in aluminum alloy powder consolidated using DC electric fields. Metall Mater Trans A. 2017;48:919–29.
10. Terauds K, Lebrun JM, Lee HH, Jeon TY, Lee SH, Je JH, et al. Electroluminescence and the measurement of temperature during Stage III of flash sintering experiments. J Eur Ceram Soc. 2015;35:3195–99.
11. Yousuf M, Sahu PCh, Rajan KG. High-pressure and high-temperature electrical resistivity of ferromagnetic transition metals: nickel and iron. Phys Rev B. 1986;34:8086–100.
12. Srivatsan TS, Narendra N, Troxell JD. Tensile deformation and fracture behavior of an oxide dispersion strengthened copper alloy. Mater Des. 2000;21:191–98.
13. Guo MX, Wang MP, Shen K, Cao LF, Tan W. Tensile fracture behavior characterization of dispersion strengthened copper alloys. J Alloys Compd. 2009;469:488–98.
14. Bamidele E, Jalali SI, Weimer AW, Raj R. Flash sintering of tungsten at room temperature (without a furnace) in < 1 min by injection of electrical currents at different rates. J. Am. Ceram. Soc. 2024;107:817–29.
15. Shewmon PG. Diffusion in solids. New York: McGraw-Hill; 1963.
16. Jalali SIA, Raj R. Reactive flash sintering in a bilayer of zirconia and lanthana: measurement of the diffusion coefficient in real time. J Am Ceram Soc. 2023;106:867–77.
17. Motomura H, Tamao D, Nambu K, Masuda H, Yoshida H. Athermal effect of flash event on high-temperature plastic deformation in Y_2O_3-stabilized tetragonal ZrO_2 polycrystal. J Eur Ceram Soc. 2022;42:5045–52.
18. Jalali SIA, Raj R. Touch-free flash sintering with magnetic induction within a reactor activated by the usual flash method. J Am Ceram Soc. 2022;105:6517–22.
19. Mishra TP, Neto RRI, Raj R, Guillon O, Bram M. Current-rate flash sintering of gadolinium doped ceria: microstructure and defect generation. Acta Mater. 2020;189:145–53.
20. Masó N, West AR. Electronic conductivity in yttria-stabilized zirconia under a small dc bias. Chem Mater. 2015;27:1552–58.
21. Jo S, Raj R. Transition to electronic conduction at the onset of flash in cubic zirconia. Scr Mater. 2020;174:29–32.
22. Jones HA. A temperature scale for tungsten. Phys Rev. 1926;28:202–7.
23. Clemenceau T, Raj R. Higher conductivity of non-stoichiometric lithium lanthanum zirconate ceramics made by reactive flash synthesis. MRS Commun. 2022;12:201–5. https://doi.org/10.1557/s43579-022-00162-z
24. Vendrell X, Yadav D, Raj R, West AR. Influence of flash sintering on the ionic conductivity of 8 mol% yttria stabilized zirconia. J Eur Ceram Soc. 2019;39:1352–58.

SUPPORTING INFORMATION

Additional supporting information can be found online in the Supporting Information section at the end of this article.

How to cite this article: Bamidele EA, Mahmoud MM, Raj R. Current rate flash sintering of nickel at ambient temperature in <1 min. J Am Ceram Soc. 2024;107:3659–65. https://doi.org/10.1111/jace.19735